

# A water-soluble, shape-persistent, mouldable supramolecular polymer with redox-responsiveness in the presence of a molecular chaperone

Xiaodong Chi,<sup>a</sup> Donghua Xu,<sup>b</sup> Xuzhou Yan,<sup>a</sup> Jianzhuang Chen,<sup>a</sup> Mingming Zhang,<sup>a</sup>  
Bingjie Hu,<sup>c</sup> Yihua Yu,<sup>c</sup> and Feihe Huang<sup>\*,a</sup>

<sup>a</sup> MOE Key Laboratory of Macromolecular Synthesis and Functionalization, Department of Chemistry, Zhejiang University, Hangzhou 310027, P. R. China; Email address: [fhuang@zju.edu.cn](mailto:fhuang@zju.edu.cn)

<sup>b</sup> State Key Laboratory of Polymer Physics and Chemistry, Changchun Institute of Applied Chemistry, Chinese Academy of Sciences, Changchun, Jilin 130022 P. R. China

<sup>c</sup> Shanghai Key Laboratory of Magnetic Resonance, Department of Physics, East China Normal University, Shanghai 200062, P. R. China

## Electronic Supplementary Information (17 pages)

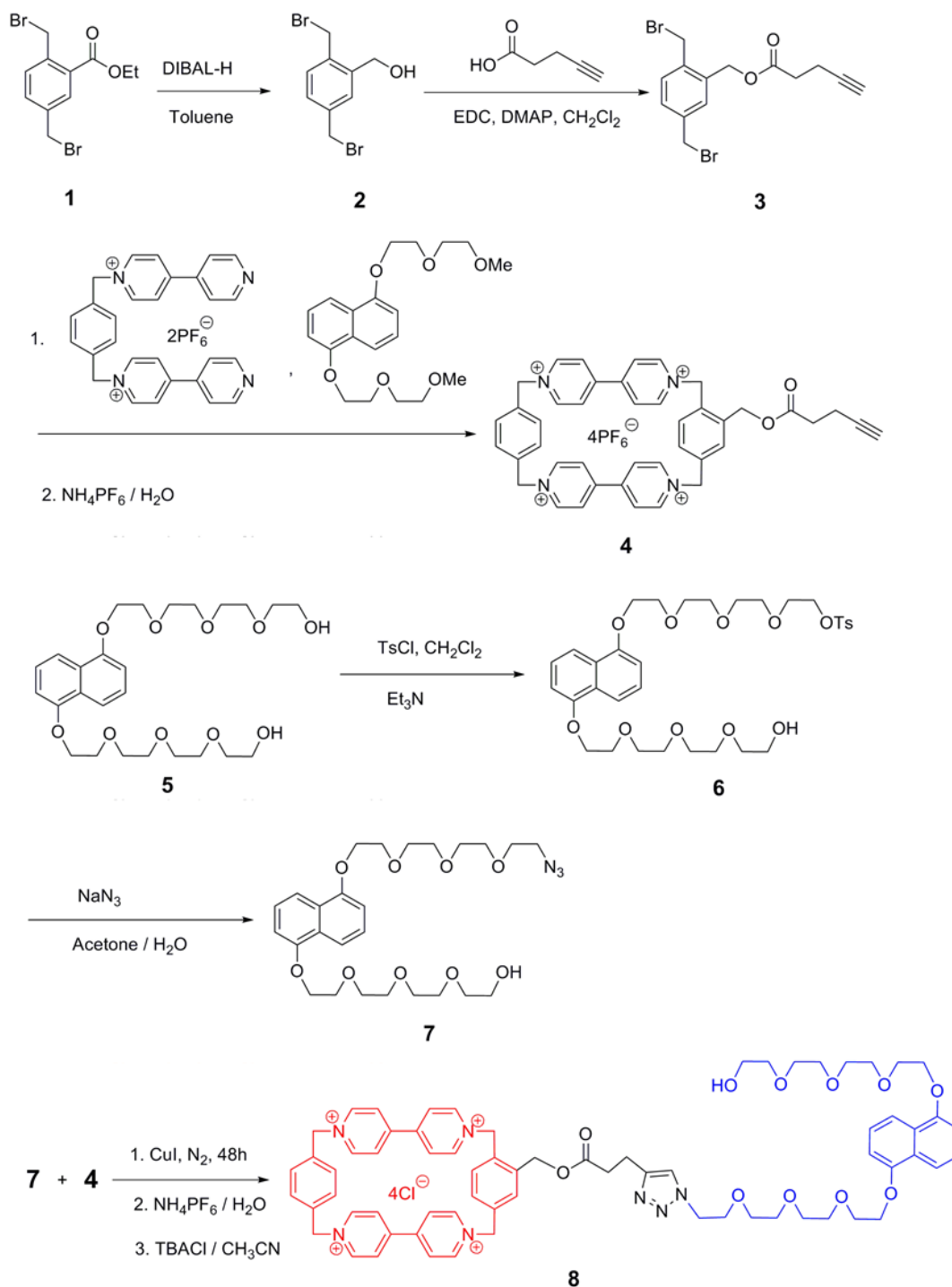
1. <i>Materials and methods</i>	S2
2. <i>Synthesis of monomer 8</i>	S3
3. <i>Partial NOESY NMR spectrum of 8</i>	S8
4. <i>Partial COSY NMR spectrum of 8</i>	S9
5. <i>The concentration-dependent <sup>1</sup>H NMR spectra of monomer 8</i>	S10
6. <i>Association constant determination for the complexation between 4 and 7</i>	S11
7. <i>Calculated values of maximum polymerization degree n at different concentrations of 8</i>	S13
8. <i>Viscosity measurements of the supramolecular polymer with different concentrations of 9</i>	S14
9. <i>DLS of the supramolecular polymer</i>	S15
10. <i>Self-healing property of the supramolecular polymer based on rheological data</i>	S16
11. <i>References</i>	S17

### 1. *Materials and methods*

All reagents were commercially available and used as supplied without further purification. Compounds **1**,<sup>S1</sup> **2**,<sup>S2</sup> **3**,<sup>S3</sup> **4**,<sup>S3</sup> **5**,<sup>S4</sup> **6**,<sup>S4</sup> and **9**<sup>S5</sup> were prepared according to the published procedures. NMR spectra were recorded with a Bruker Avance DMX 500 spectrophotometer or a Bruker Avance DMX 400 spectrophotometer using the deuterated solvent as the lock and the residual solvent or TMS as the internal reference. Low-resolution electrospray ionization mass spectra were recorded with a Bruker Esquire 3000 Plus spectrometer. High-resolution mass spectrometry experiments were performed with a Bruker Daltonics Apex III spectrometer. Viscosity measurements were carried out with a Cannon-Ubbelohde semi-micro dilution viscometer at 298 K in water. The two-dimensional diffusion-ordered NMR spectra were recorded on a Bruker DRX500 spectrometer. Scanning electron microscopy investigations were carried out on a JEOL 6390LV instrument. The melting points were collected on a SHPSIC WRS-2 automatic melting point apparatus. UV-Vis spectroscopy was performed on a Shimadzu UV-2550 instrument at room temperature. Dynamic light scattering (DLS) measurements were carried out using a 200-mW polarized laser source Nd : YAG ( $\lambda = 532$  nm). The polarized scattered light was collected at 90° in a self-beating mode with a Hamamatsu R942/02 photomultiplier. The signals were sent to a Malvern 4700 submicrometer particle analyzer system. Rheological data were obtained by using an ARES G2 rheometer (TA Instruments) with parallel plate geometry (diameter of 8 mm). Strain sweep was performed from small to large strain at 10 rad/s. Oscillatory frequency sweep experiments were performed at 298 K from 0.1 rad/s to 300 rad/s with a strain in the linear region.

## 2. Synthesis of monomer 8

**Scheme S1. Synthesis of monomer 8**



Compound **7**: A solution of **6** (1.20 g, 1.80 mmol) and  $\text{NaN}_3$  (0.40 g, 3.6 mmol) in acetone/ $\text{H}_2\text{O}$  (120 mL,  $v : v = 5:1$ ) was stirred at room temperature for about 12 h. Then the solvent was evaporated under reduced pressure and the residue was dissolved in  $\text{CH}_2\text{Cl}_2$ . The resultant solution was washed with  $\text{H}_2\text{O}$  and brine. The

organic phase was collected, dried over anhydrous  $\text{Na}_2\text{SO}_4$  and concentrated to give **7** (0.97 g, 100%) as a light yellow oil. The proton NMR spectrum of **7** is shown in Fig. S1.  $^1\text{H}$  NMR (400 MHz,  $\text{CDCl}_3$ , 298 K)  $\delta$  (ppm): 7.74 (d,  $J = 8$  Hz, 2H), 7.21 (t,  $J = 8$  Hz, 2H), 6.68 (d,  $J = 8$  Hz, 2H), 4.10 (m, 4H), 3.81–3.78 (m, 4H), 3.62–3.58 (m, 4H), 3.55–3.38 (m, 18H), 3.17–3.14 (m, 2H). The  $^{13}\text{C}$  NMR spectrum of **7** is shown in Fig. S2.  $^{13}\text{C}$  NMR (125 MHz,  $\text{CDCl}_3$ , 298 K)  $\delta$  (ppm): 154.27, 154.25, 126.65, 125.08, 114.52, 105.59, 77.76, 77.51, 77.25, 72.49, 70.83, 70.79, 70.61, 70.54, 70.50, 70.48, 70.17, 69.87, 69.65, 67.80, 61.45, 50.51. LRESIMS is shown in Fig. S3:  $m/z$  560.2 [ $\text{M} + \text{Na}$ ] $^+$ , HRESIMS:  $m/z$  calcd for [ $\text{M} + \text{Na}$ ] $^+$   $\text{C}_{26}\text{H}_{39}\text{N}_3\text{O}_9\text{Na}^+$ , 560.2579; found 560.2569, error  $-1.7$  ppm.

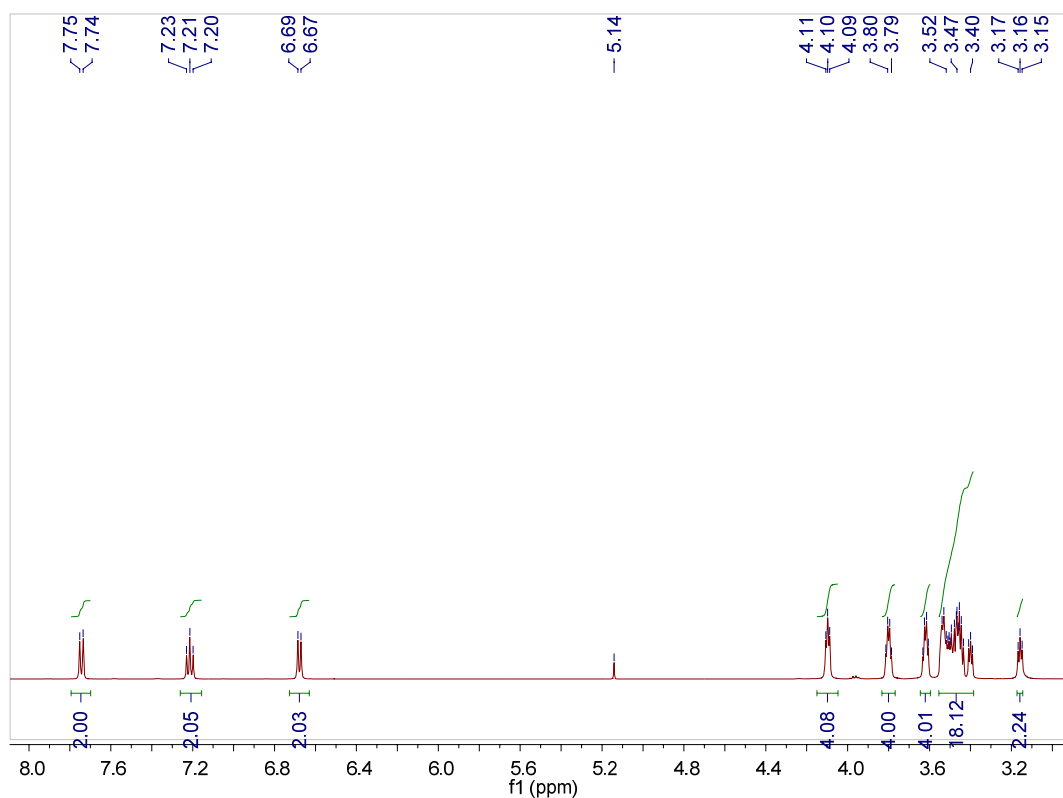


**Fig. S1.**  $^1\text{H}$  NMR spectrum (400 MHz, chloroform-*d*, room temperature) of **7**.

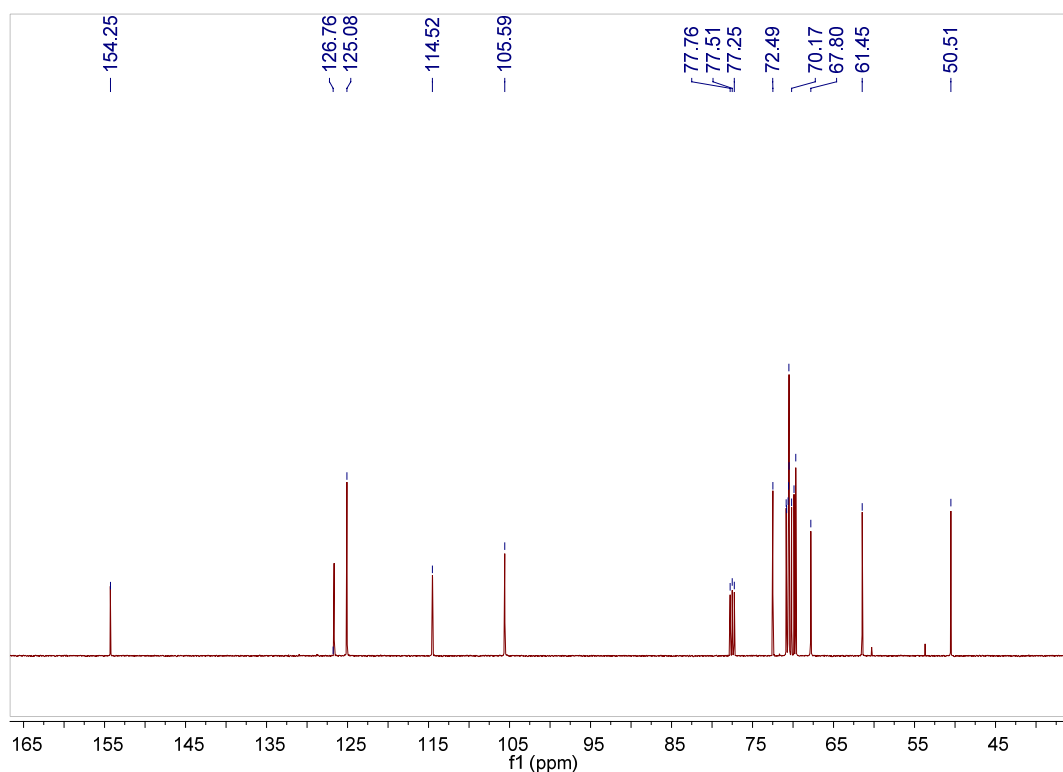


**Fig. S2.**  $^{13}\text{C}$  NMR spectrum (100 MHz, chloroform-*d*, room temperature) of **7**.

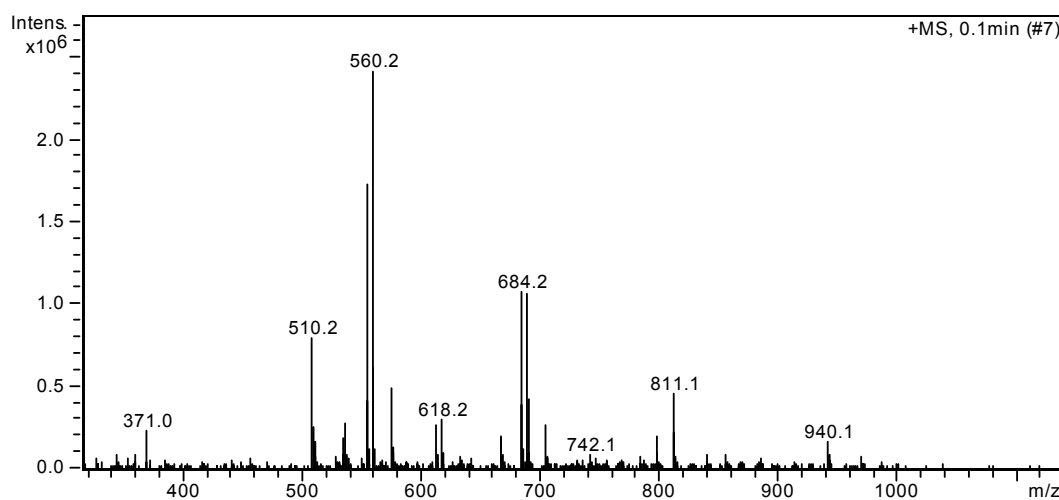


**Fig. S3.** Electrospray ionization mass spectrum of **7**.

*Compound 8*: A mixture of **4** (0.40 g, 0.33 mmol), **7** (0.18 g, 0.33 mmol) and CuI (7.0 mg, 0.033 mmol) was stirred under  $\text{N}_2$  at room temperature for 2 days. After the removal of the solvent under reduced pressure, the residue was subjected to column chromatography (methanol /  $\text{NH}_4\text{Cl}$  (2 M) /  $\text{MeNO}_2$ , 7:2:1 v/v/v). The fraction containing the product was collected and concentrated under reduced pressure. The

residue was dissolved in hot water and a saturated solution of  $\text{NH}_4\text{PF}_6$  was added. The precipitate was collected by filtration and washed with water to provide a purple solid. Then excess tetrabutylammonium chloride (TBACl) was added to a solution of the above purple solid in  $\text{CH}_3\text{CN}$ . Some purple solid was precipitated, which was collected by filtration and washed by  $\text{CH}_3\text{CN}$  to afford **8** (0.43 g, 90%) as a red solid, m.p. > 270 °C. The proton NMR spectrum of **8** is shown in Fig. S4.  $^1\text{H}$  NMR (500 MHz,  $\text{D}_2\text{O}$ , 298 K)  $\delta$  (ppm): 9.21–8.61 (m, 8H), 8.41–7.66 (m, 8H), 7.64–7.24 (m, 8H), 6.45–5.38 (m, 14H), 4.51–4.10 (m, 10H), 3.94 (m, 8H), 3.82–3.50 (m, 10H), 3.43–3.33 (m, 4H), 3.23 (m, 1H), 3.06–2.74 (m, 4H), 2.59–2.35 (m, 2H). The  $^{13}\text{C}$  NMR spectrum of **8** is shown in Fig. S5.  $^{13}\text{C}$  NMR (125 MHz,  $\text{D}_2\text{O}$ , 298 K)  $\delta$  (ppm): 173.53, 173.24, 150.34, 145.35, 144.53, 144.22, 143.72, 142.78, 135.54, 134.12, 133.27, 132.78, 130.33, 127.66, 127.47, 125.11, 124.03, 123.83, 122.41, 118.23, 107.61, 103.49, 70.72, 69.99, 69.49, 69.31, 68.99, 68.65, 68.48, 67.66, 67.04, 64.44, 59.29, 57.20, 48.60, 32.14, 31.99, 22.23, 19.57, 18.25, 11.95. LRESIMS is shown in Fig. S6:  $m/z$  1273.6  $[\text{M} - \text{Cl} + \text{H}]^+$ , 619.5  $[\text{M} - 2\text{Cl} + \text{H}]^{2+}$ . HRESIMS:  $m/z$  calcd for  $[\text{M} - \text{Cl}]^+ \text{C}_{68}\text{H}_{77}\text{N}_7\text{O}_{11}\text{Cl}_3^+$ , 1272.4747; found 1272.4752, error 0.4 ppm.

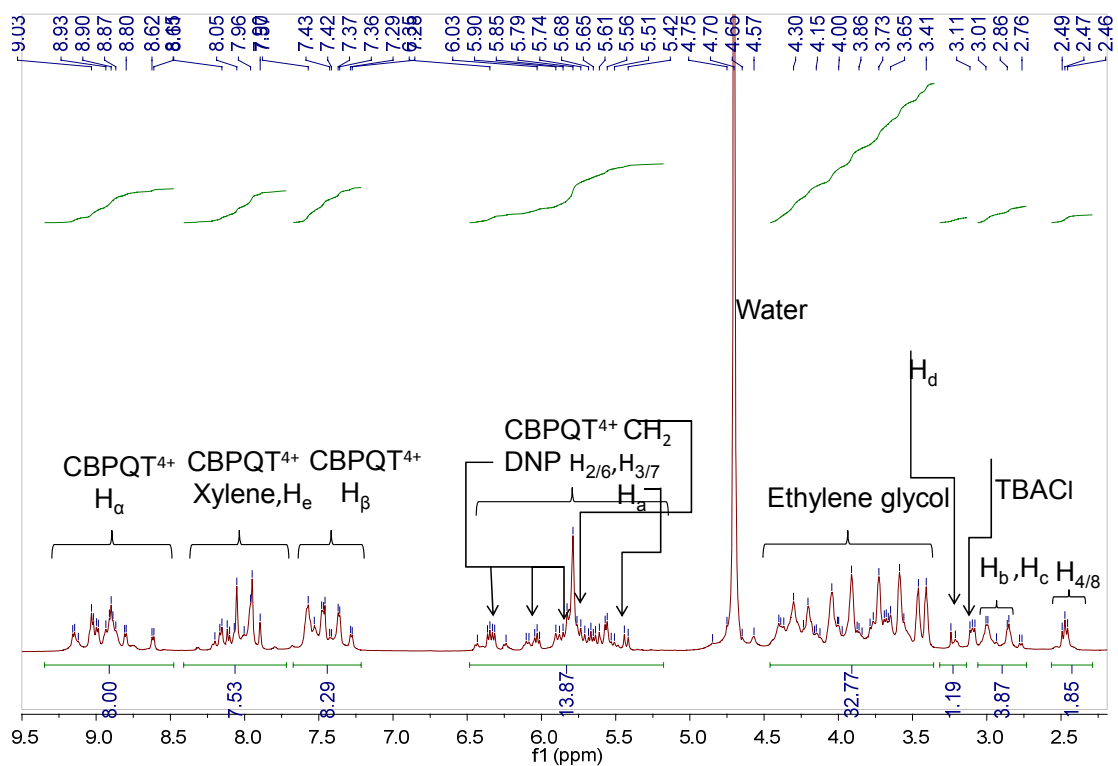


**Fig. S4.** <sup>1</sup>H NMR spectrum (500 MHz, D<sub>2</sub>O, room temperature) of **8**.

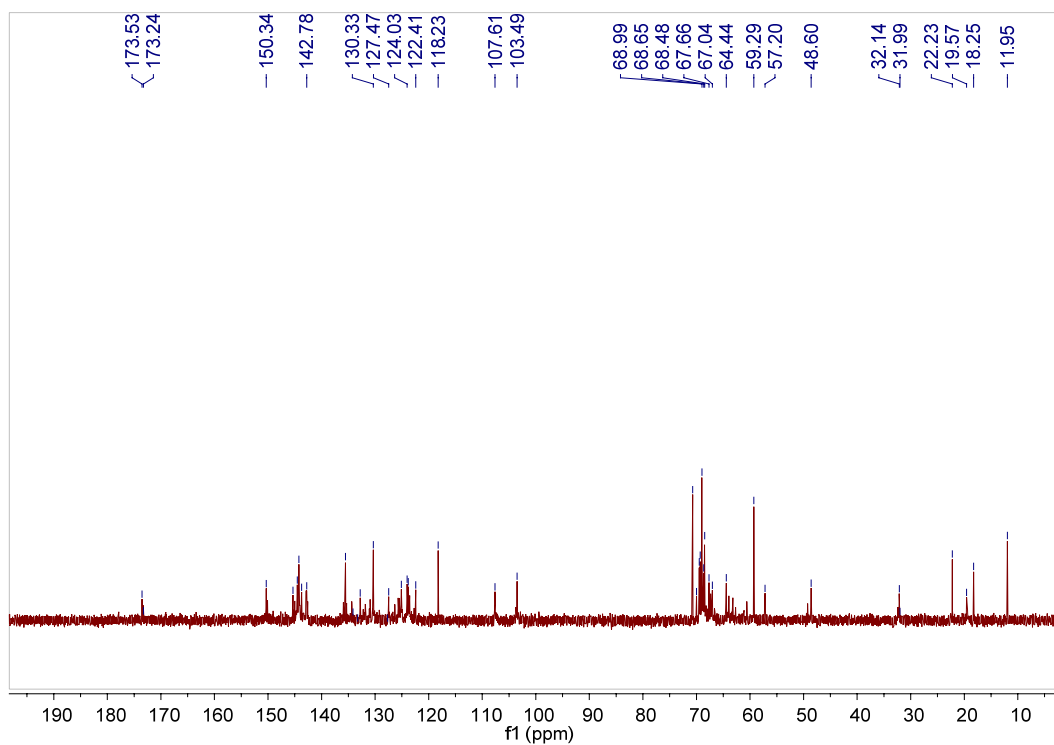


**Fig. S5.** <sup>13</sup>C NMR spectrum (125 MHz, D<sub>2</sub>O, room temperature) of **8**.

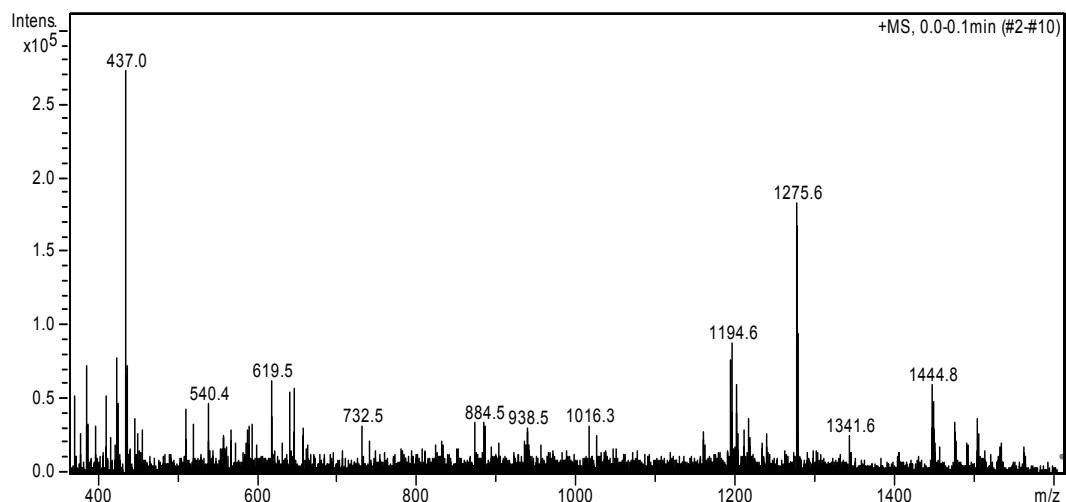


**Fig. S6.** Electrospray ionization mass spectrum of **8**.

### 3. Partial NOESY NMR spectrum of **8**

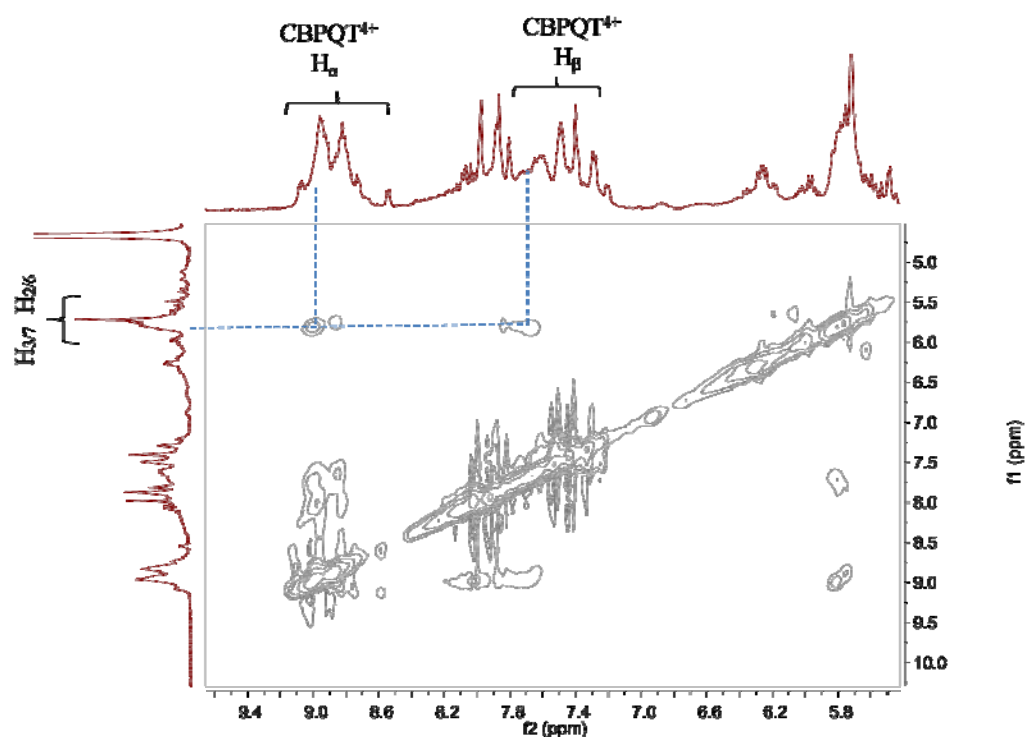


**Fig. S7.** Partial NOESY NMR (400 MHz, D<sub>2</sub>O, 298 K) spectrum of a solution of **8** at a concentration of 30.0 mM. From this NOESY NMR spectrum, strong correlations were observed between protons H<sub>α</sub> and H<sub>β</sub> of CBPQT<sup>4+</sup> and protons H<sub>3/7</sub> and H<sub>2/6</sub> of DNP, confirming the occurrence of CBPQT<sup>4+</sup>/DNP complexation in water.

4. Partial COSY NMR spectrum of **8**

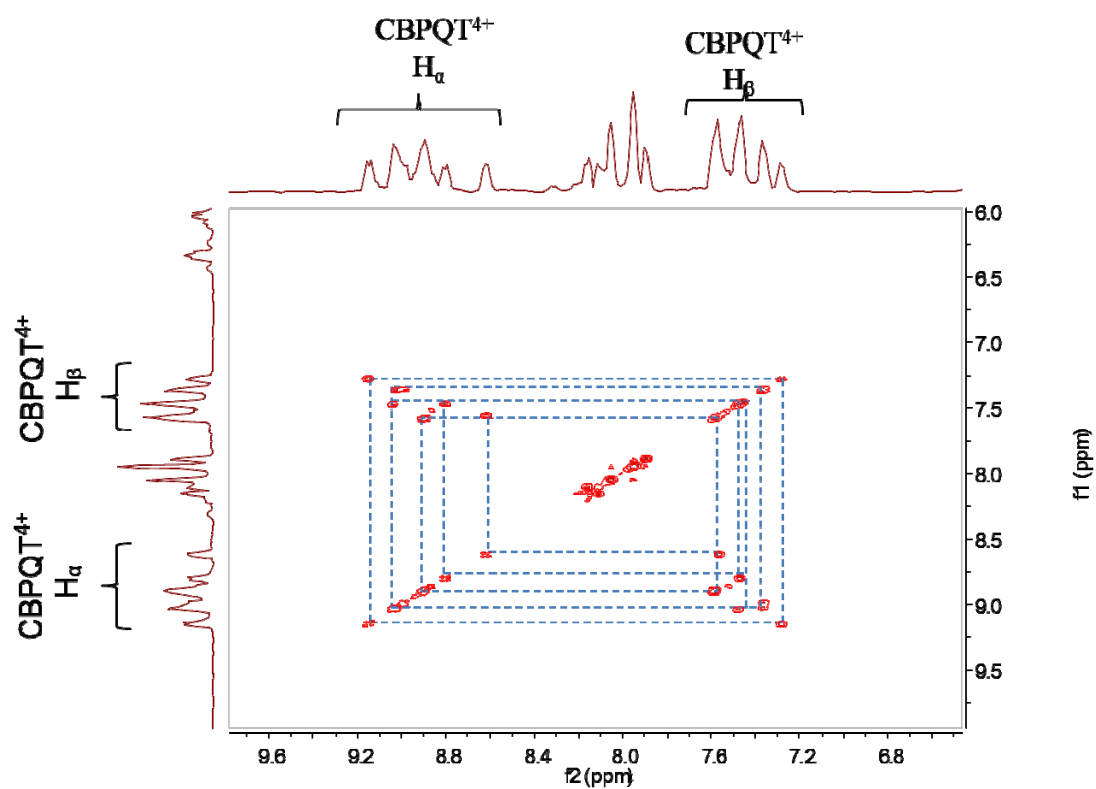


**Fig. S8.** Partial COSY NMR (500 MHz,  $\text{D}_2\text{O}$ , 298 K) spectrum of a solution of **8** at a concentration of 30.0 mM.

5. The concentration-dependent  $^1\text{H}$  NMR spectra of monomer **8**

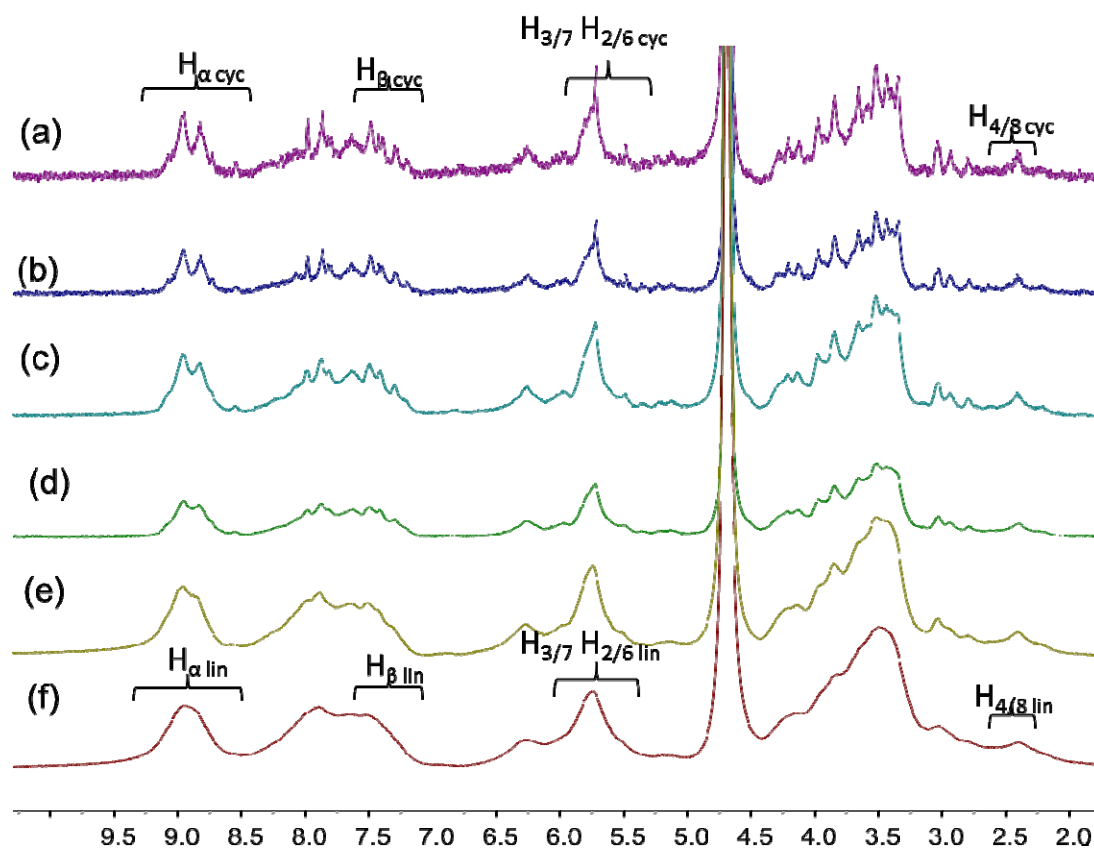


**Fig. S9.** Partial  $^1\text{H}$  NMR spectra (400 MHz,  $\text{D}_2\text{O}$ , 298 K) of monomer **8** at different concentrations: (a) 5.00 mM, (b) 20.0 mM, (c) 50.0 mM, (d) 80.0 mM, (e) 100 mM, (f) 120 mM. Due to the slow complexation between the  $\text{CBPQT}^{4+}$  host unit and the DNP guest moiety and the existence of too many peaks, these spectra are very complicated, making it impossible to tell which peaks belong to complexed and uncomplexed species. The peaks are sharp at low concentration while they are broad at high concentration, indicating the formation of a supramolecular polymer with the increasing concentration.

### 6. Association constant determination for the complexations between **4** and **7**

The association constant of complex **4** ⊃ **7** was determined by probing the charge-transfer band of the complex by UV-Vis spectroscopy and employing a titration method. Progressive addition of an aqueous solution with high host **4** concentration and low guest **7** concentration to an aqueous solution with the same concentration of guest **7** resulted in an increase of the intensity of the charge-transfer band of the complex. Treatment of the collected absorbance data at  $\lambda = 520$  nm with a non-linear curve-fitting program afforded the corresponding association constant ( $K_a$ ),  $(3.2 \pm 0.3) \times 10^3 \text{ M}^{-1}$ , for **4** ⊃ **7**.

The non-linear curve-fitting was based on the equation:<sup>S6</sup>

$$A = (A_\infty/[G]_0) (0.5[H]_0 + 0.5([G]_0 + 1/K_a) - (0.5([H]_0^2 + 2[H]_0(1/K_a - [G]_0) + (1/K_a + [G]_0)^2)^{0.5})) \text{ (Eq. S1)}$$

Where A is the absorption intensity of the charge-transfer band ( $\lambda = 520$  nm) at  $[H]_0$ ,  $A_\infty$  is the absorption intensity of the charge-transfer band ( $\lambda = 520$  nm) when the guest is completely complexed,  $[G]_0$  is the fixed initial concentration of the guest, and  $[H]_0$  is the initial concentration of the host.

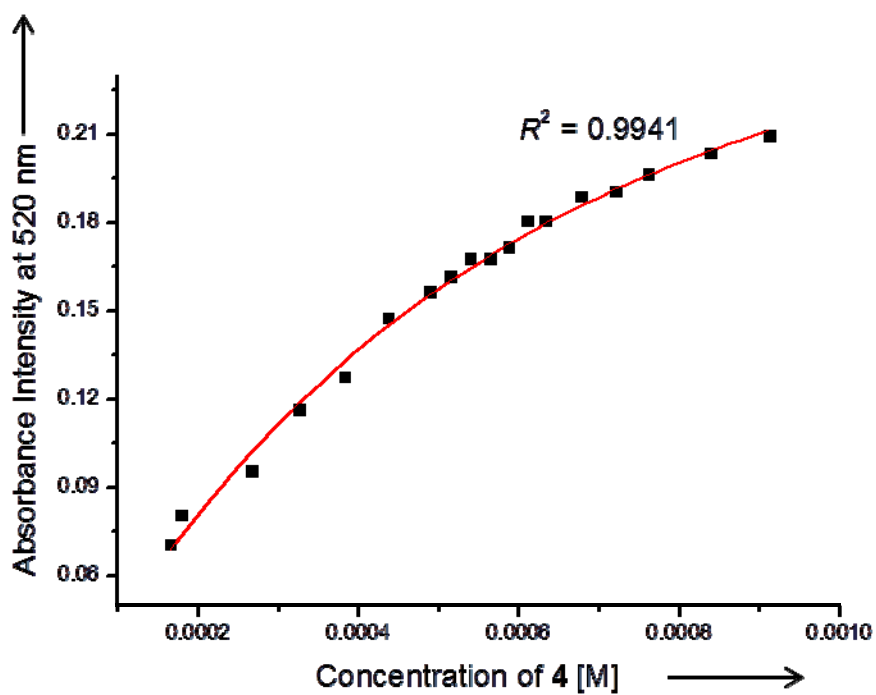
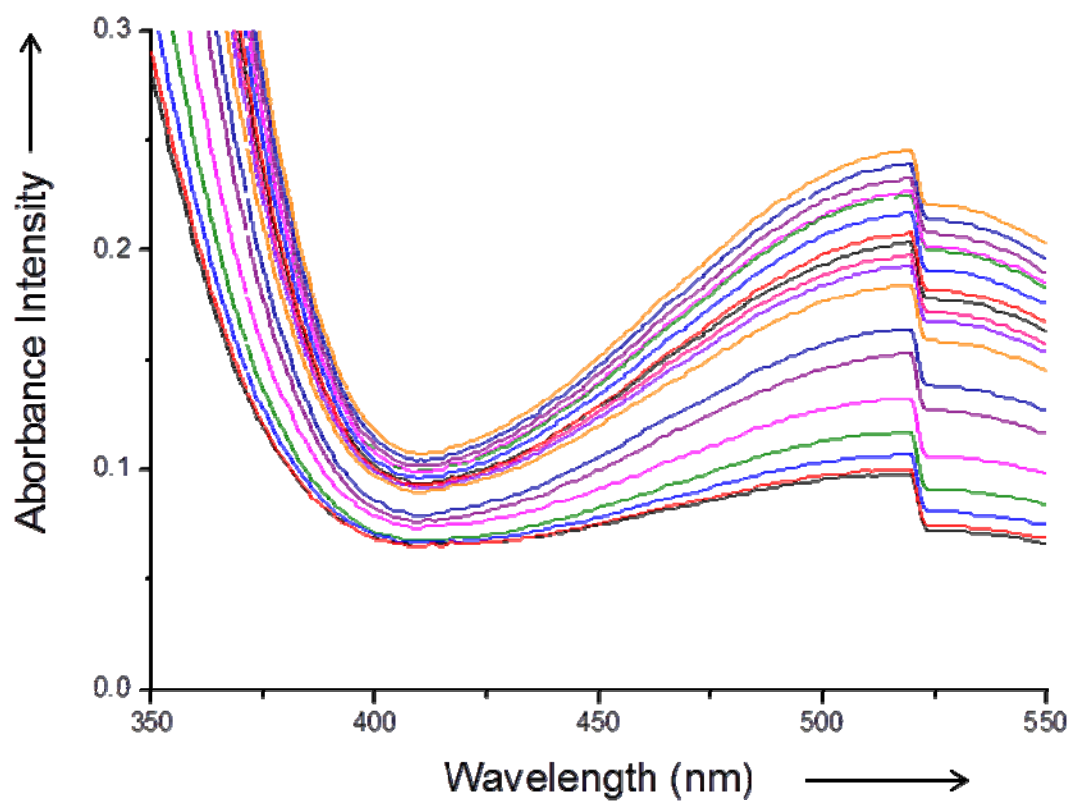


**Fig. S10.** Titration curve (top) and non-linear fitting curve (bottom) of host 4 and guest 7.

### 7. Calculated values of maximum polymerization degree $n$ at different concentrations of **8**

Using the Carothers equation and assuming that the same average association constant holds for each successive step (isodesmic) and that cyclic species can either be ignored or taken into account, the average degree of polymerization,  $n$ , is easily derived as being related to the equilibrium constant  $K_a$  and the initial monomer concentration as follows:<sup>S7</sup>

If we now define  $p$  = extent of complexation,

$$K_a = p[H]_0 / (1 - p)^2 [H]_0^2.$$

Solving this quadratic equation leads to

$$1 - p = \{(1 + 4K_a[H]_0)^{1/2} - 1\} / 2K_a[H]_0$$
$$n = 1/(1 - p) = 2K_a[H]_0 / \{(1 + 4K_a[H]_0)^{1/2} - 1\} \quad (1)$$

if  $4K_a[H]_0 \gg 1$ ,  $n = 2K_a[H]_0 / \{(4K_a[H]_0)^{1/2} - 1\}$  and

$$\text{if } (4K_a[H]_0)^{1/2} \gg 1, n = (K_a[H]_0)^{1/2} \quad (2)$$

In this system  $p$  is the extent of complexation and  $[H]_0 = [\mathbf{8}]_0$ . Therefore, degrees of polymerization calculated in this way represent maximum values that in practice will be reduced by formation of cyclics and possibly by reduction in the association constant as the suprapolymer grows (“attenuation”). As the concentration increases, the calculated size of aggregates increases to large values. For example, at 150 mM,  $p = 95.6\%$  and  $n = 22.4$ , corresponding to a polymer with a molar mass of 29.3 kDa.

Table S1. Calculated values of  $p$  and  $n$  at different concentrations of monomer **8**.

[monomer <b>8</b> ] <sub>0</sub> (mM)	$p$	$n_{\max}$
1.00	0.355	2.6
5.00	0.783	4.6
30.0	0.902	10
50.0	0.924	13
90	0.943	17
150	0.956	22
200	0.962	26
300	0.968	32

8. Viscosity measurements of the supramolecular polymer with different concentrations of **9**

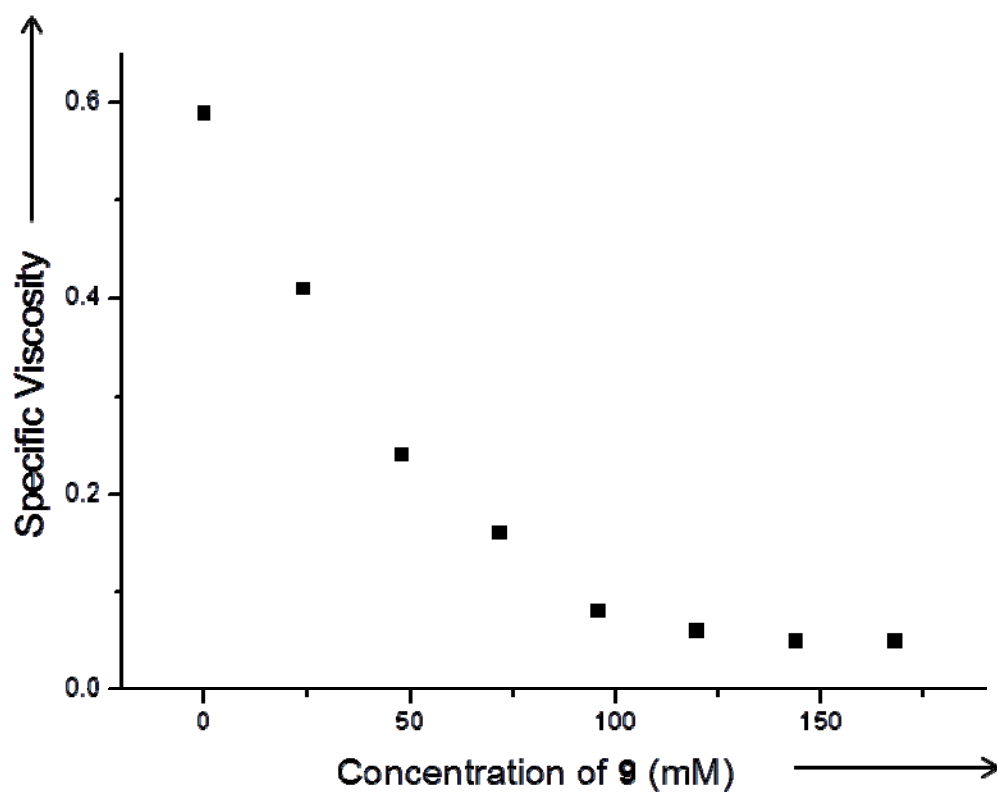
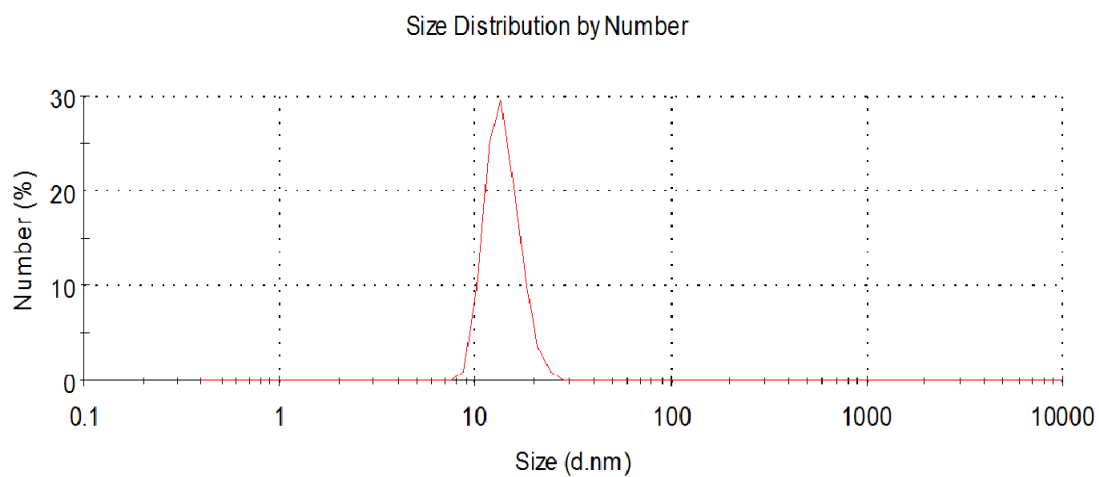


Fig. S11. Specific viscosity of monomer **8** (120 mM) with different concentrations of **9**.

### 9. DLS of the supramolecular polymer

The solutions were filtered through a Teflon filter (pore size: 0.22  $\mu\text{m}$ ), prior to use. An 80.0 mM solution of **8** in  $\text{H}_2\text{O}$  has a hydrodynamic radius of 13.5 nm, while no aggregate was detected for a 10.0 mM solution of **8**.



**Fig. S12.** Hydrodynamic radius ( $R_H$ ) of a 80.0 mM solution of **8** measured by DLS.

10. Self-healing property of the supramolecular polymer based on rheological data

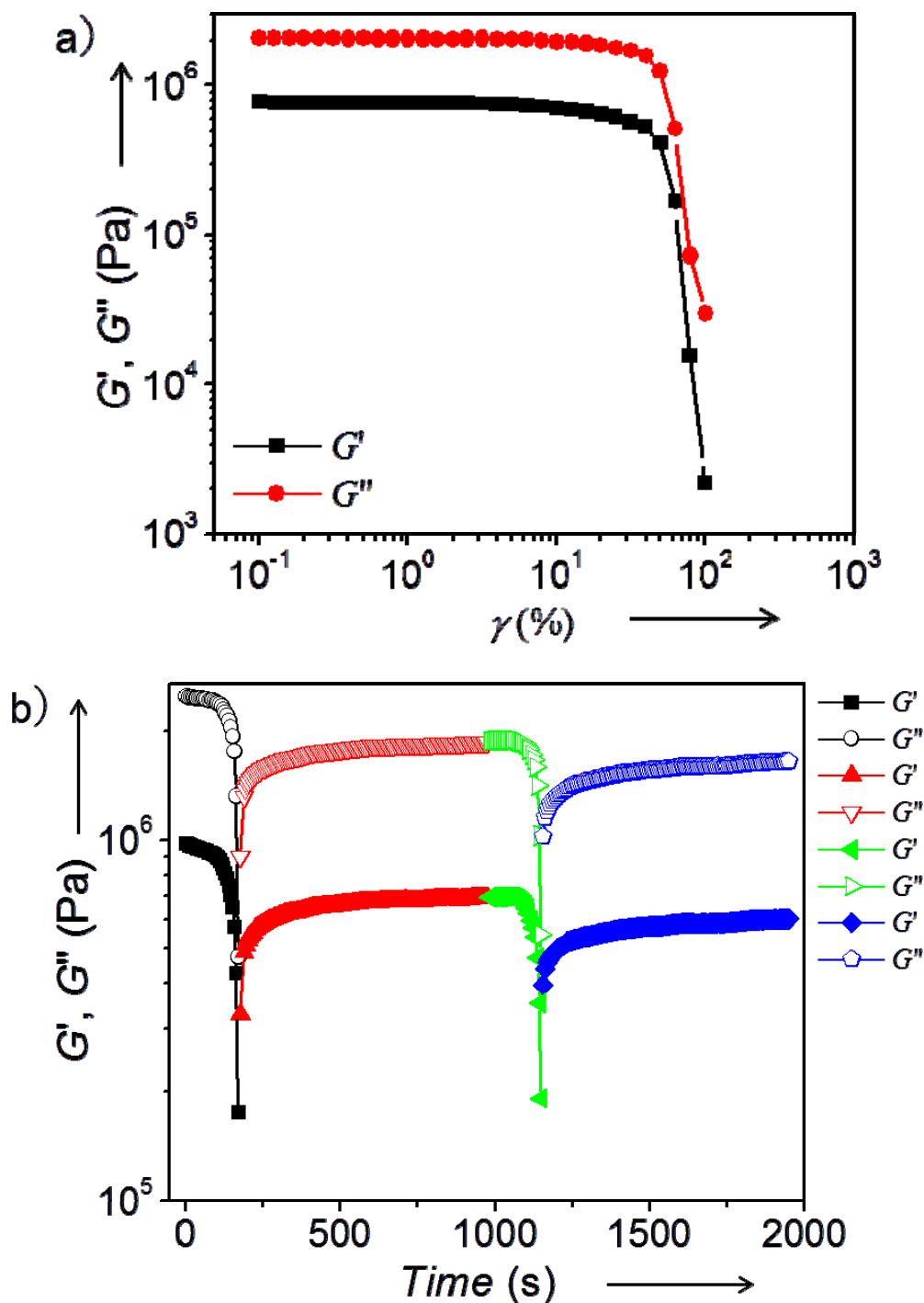


**Fig. S13.** (a)  $G'$  and  $G''$  values of a sample made from monomer **8** by using 400 mg of monomer **8** and 0.200 mL of H<sub>2</sub>O during strain sweep at 10 rad/s; (b)  $G'$  and  $G''$  values of the above sample during time sweep. Time-dependent strain sweep from 0.1% to 63% and then back to 0.5% strain for 800 s at a scan frequency of 10 rad/s. And another cycle was done.  $T = 298$  K.

According to the strain sweep results of the sample made from monomer **8** by using 400 mg of monomer **8** and 0.200 mL of H<sub>2</sub>O (Fig. S13a), as the strain is larger than 40%, the sample is in the nonlinear strain regime. Both  $G'$  and  $G''$  of the sample decrease rapidly when strain is larger than 40%, indicating that sample is partly broken under larger strain (> 40%). In Fig. S13b, during the strain sweep of the sample from 0.1% to 63% strain at 10 rad/s, the breakage of network at larger strain is apparent as  $G'$  and  $G''$  start to drop rapidly. During the following time sweep experiments at 0.5% strain (linear strain regime) for 800 s at 10 rad/s, the rapid recovery of the network structure is also apparent as  $G'$  and  $G''$  start to increase rapidly at the beginning. However, only partial recovery of  $G'$  and  $G''$  of the sample was achieved. The results in Fig. S13b illustrated that the supramolecular polymer material has self-healing properties to a certain degree.

#### 11. References:

- S1. P. R. Ashton, R. Ballardini, V. Balzani, S. E. Boyd, A. Credi, M. T. Gandolfi, M. Gomez-Lopez, S. Iqbal, D. Philp, J. A. Preece, L. Prodi, H. G. Ricketts, J. F. Stoddart, M. S. Tolley, M. Venturi, A. J. P. White and D. J. Williams, *Chem. Eur. J.*, 1997, **3**, 152.
- S2. G. Cooke, P. Woisel, M. Bria, F. Delattre, J. F. Garety, S. G. Hewage, G. Rabani and G. M. Rosair, *Org. Lett.*, 2006, **8**, 1423.
- S3. M. Bria, J. Bigot, G. Cooke, J. Lyskawa, G. Rabani, V. M. Rotello and P. Woisel, *Tetrahedron*, 2009, **65**, 400.
- S4. O. Š. Miljanic, W. R. Dichtel, S. L. Khan, S. Mortezaei, J. R. Heath and J. F. Stoddart, *J. Am. Chem. Soc.*, 2007, **129**, 8236.
- S5. L. R. Melby, H. D. Hartzler and W. A. Sheppard, *J. Org. Chem.*, 1974, **39**, 2456.
- S6. (a) K. A. Connors, *Binding Constants*, Wiley: New York, 1987; (b) P. S. Corbin, Ph.D. Dissertation, University of Illinois at Urbana-Champaign, Urbana, IL, 1999; (c) P. R. Ashton, R. Ballardini, V. Balzani, M. Bělohradský, M. T. Gandolfi, D. Philp, L. Prodi, F. M. Raymo, M. V. Reddington, N. Spencer, J. F. Stoddart, M. Venturi and D. J. Williams, *J. Am. Chem. Soc.*, 1996, **118**, 4931.
- S7. H. W. Gibson, N. Yamaguchi and J. W. Jones, *J. Am. Chem. Soc.*, 2003, **125**, 3522.